Accepted Manuscript

Mechanical and tribological behavior of Ti/TiN and TiAl/TiAlN coated austempered ductile iron

Diego A. Colombo, Alejo D. Mandri, María D. Echeverría, Juan M. Massone, Ricardo C. Dommarco

PII: S0040-6090(17)30910-0
DOI: https://doi.org/10.1016/j.tsf.2017.12.014
Reference: TSF 36388

To appear in: *Thin Solid Films*

Received date: 4 September 2017
Revised date: 22 November 2017
Accepted date: 16 December 2017

Please cite this article as: Diego A. Colombo, Alejo D. Mandri, María D. Echeverría, Juan M. Massone, Ricardo C. Dommarco , Mechanical and tribological behavior of Ti/TiN and TiAl/TiAlN coated austempered ductile iron. The address for the corresponding author was captured as affiliation for all authors. Please check if appropriate. Tsf(2017), https://doi.org/10.1016/j.tsf.2017.12.014

This is a PDF file of an unedited manuscript that has been accepted for publication. As a service to our customers we are providing this early version of the manuscript. The manuscript will undergo copyediting, typesetting, and review of the resulting proof before it is published in its final form. Please note that during the production process errors may be discovered which could affect the content, and all legal disclaimers that apply to the journal pertain.

ACCEPTED MANUSCRIPT

Mechanical and tribological behavior of Ti/TiN and TiAl/TiAlN coated austempered ductile iron

Diego A. Colombo*, Alejo D. Mandri, María D. Echeverría, Juan M. Massone, Ricardo C. Dommarco

Instituto de Investigaciones en Ciencia y Tecnología de Materiales, UNMdP, CONICET, Facultad de Ingeniería, Av. J. B. Justo 4302, B7608FDQ Mar del Plata, Argentina

* Corresponding author:

Phone: +54-223-481-6600 ext. 260

Fax: +54-223-481-0046

E-mail address: diegocolombo@fi.mdp.edu.ar

ACCEPTED MANUSCRIPT

Abstract

Bilayer Ti/TiN and TiAl/TiAlN coatings were deposited onto austempered ductile iron (ADI) substrates by cathodic arc deposition in an industrial device. Structure and mechanical properties of the coated samples were comparatively examined. Wear behavior of the coated samples was investigated in comparison with uncoated ADI by means of rolling contact fatigue (RCF) tests, performed in a flat washer type testing rig and using lubricated

ACCEPTED MANUSCRIPT

pure rolling conditions. RCF tests results were analyzed using the two-parameter Weibull distribution and the Weibayes method.

The results indicate that TiN and TiAlN coatings grew with a cubic-NaCl type structure. The arithmetic average roughness of the coated samples is similar for both coating variants. The surface hardness and residual stresses are higher for the TiAl/TiAlN coated samples. The coating hardness and elastic modulus are also higher for TiAl/TIAlN. The critical loads at massive delamination and the evolution of the friction coefficients are quite similar for both coating variants. Regarding RCF, failures in coated samples were characterized by substrate spalling. No massive delamination was observed in Ti/TiN and TiAl/TiAlN coatings. The statistical analysis indicates that the deposition of Ti/TiN improves noticeably the RCF resistance of ADI while the deposition of TiAl/TiAlN does not produce significant changes. The properties mismatch between substrate and coating seems to play an important role in the RCF behavior of coated samples, since Ti/TiN coatings possess a lower mismatch with respect to ADI substrates as compared to TiAl/TiAlN.

Keywords

Austempered ductile iron; Cathodic arc deposition; Titanium; Titanium nitride; Titanium aluminum nitride; Titanium aluminide; Mechanical properties; Wear behavior

1. Introduction

ACCEPTED MANUSCRIPT

ACCEPTED MANUSCRIPT

Austempered ductile iron (ADI) is an attractive engineering material because of its excellent combination of high strength and ductility with good wear resistance. In addition, the manufacturing cost and density of ADI are lower than forged or cast steels. Therefore, it is considered as an economical substitute for steel castings and forgings in many structural applications. However, due to its intrinsic microstructural nature, ADI tends to be less resistant to rolling contact fatigue (RCF) than steels, since graphite nodules act as preferential sites for crack nucleation. Consequently, the use of surface treatments could offset the negative effect of the nodules.

In previous works, the authors of this paper studied the RCF behavior of ADI samples coated with monolayer and bilayer films deposited by cathodic arc deposition (CAD) using industrial and experimental devices, respectively [1-3]. It was found that the resistance of the monolayer coated samples increases as coating hardness and thickness decrease. In addition, the predominant failure mode of the coated samples changes from substrate spalling to coating delamination as coating thickness increases. Regarding bilayer coatings it was found that, as the RCF tests go forward, the outer layer is progressively delaminated while the interlayer remains adhered to the substrate until final failure by substrate spalling occurred. However, no significant changes between the RCF life of the samples with monolayer and bilayer coatings were observed.

It is well known that conventional binary transition metal nitride coatings, such as TiN, can be alloyed with a third element, e.g. Al, Zr, C and Si, to improve the properties of the coating [4-7]. Over the last decades, TiAlN coatings are increasingly drawing attention because of their outstanding properties, such as high hardness, good wear resistance and

ACCEPTED MANUSCRIPT

excellent oxidation resistance [6, 8-10]. More recently, it has been proven that the performance of TiAlN coatings depends strongly on the Al/Ti ratio. Increasing the Al content has a beneficial effect on the mechanical properties and oxidation resistance [11, 12]. However, the crystal structure of $Ti_{1-x}Al_xN$ changes from the cubic-NaCl type to the wurtzite-ZnS type at an Al content x = 0.6 (mol fraction), and thereby causes a decrease in hardness and elastic modulus as well as in wear resistance [11-14]. For that reason, TiAlN coatings with cubic structure have been used for practical purposes so far.

On this basis, the aim of this work is to study the properties and RCF behavior of ADI samples coated with bilayer TiAl/TiAlN films synthesized by CAD using an industrial device. Bilayer Ti/TiN coatings are also analyzed for comparative purposes.

2. Experimental procedures

2.1 Substrate material and samples preparation

The ductile iron was produced in an induction furnace, conventionally nodulized and inoculated [15] and then it was poured into horizontal sand moulds designed to obtain discs with 70 mm in diameter and 10 mm in thickness.

The chemical composition of the obtained material (wt. %), analyzed by optical emission spectrometry, was 3.35 % C; 2.87 % Si; 0.13 % Mn; 0.015 % S; 0.032 % P; 0.043 % Mg; 0.76 % Cu; 0.57 % Ni and Fe balanced. The nodule count of the samples was about 300

ACCEPTED MANUSCRIPT

nod/mm^2, with an average nodule diameter of 20 µm. Nodularity exceeded 90 % in all cases according to the ASTM A247 standard.

The discs were cut from the castings, then machined by turning to obtain samples with a final size of 65 mm in diameter and about 8 mm in thickness, and finally heat treated to obtain a high resistance ADI grade. The heat treatment consisted in an austenitising at 910 °C for 120 min, an austempering in a salt bath at 280 °C for 90 min, and a subsequent air cooling to room temperature. The average Brinell hardness was 420 $HBW_{2.5/187.5}$.

ADI samples were finished by conventional surface grinding, carried out in a horizontal-spindle surface grinder and under industrial-use cutting conditions. Three roughing passes and one finishing pass were conducted on each sample. The finishing pass aims to attain a low surface roughness. A vitrified wheel with SiC abrasive grains was employed. A 5 % aqueous solution of soluble oil was used as cooling fluid.

2.2. Coating process

The coatings were synthesized by CAD using an industrial PVD device. All the substrates were degreased, ultrasonically cleaned, rinsed with alcohol, and dried by warm air prior to deposition. Once inside the coating chamber, the substrates were cleaned again by bombardments with energetic ions from the target for 10 minutes. During cleaning the substrates were biased at -1000 V and the chamber pressure was maintained at $2x10^{-3}$ Pa. The substrates were mounted on a holder located at 200 mm from the cathode front surface and kept at 300 °C. The depositions were carried out with a discharge current of

ACCEPTED MANUSCRIPT

60 A. During the process the substrates were biased at -175 V respect to the anode and the chamber pressure was maintained at 2 Pa.

Ti/TiN and TiAl/TiAlN coatings were synthesized using 99.99 % pure Ti and TiAl (50:50 at. %) targets, respectively. The total thickness of the coatings was intended to be about 1.2 µm. The average deposition rate turned out to be 0.020 ± 0.004 µm/min for both coating variants. Thereby, a total deposition time of 60 minutes was selected. Ti and TiAl were first deposited for 10 minutes, serving as interlayers. Then, nitrogen was injected to the chamber to deposit TiN and TiAlN for 50 minutes. According to previous studies [16], the temperature-time combination used for the depositions does not produce noticeably changes in the ausferritic structure.

2.3. Substrates and coatings characterization

Phase identification in the uncoated and coated samples was performed by x-ray diffraction (XRD). A Phillips XPERT-PRO diffractometer with Cu Kα radiation (λ = 1.5418 Å) was utilized. XRD patterns were recorded in a 2θ range from 30° to 90°.

The conventional arithmetic average roughness (*Ra*) of the uncoated and coated samples was analyzed using a stylus profilometer (Taylor Hobson Surtronic 3+) with a 4 mm evaluation length (cut-off, 0.8 mm). A microindentation tester equipped with a Knoop indenter was used to measure the surface hardness (15 g load) of the uncoated and coated samples.

ACCEPTED MANUSCRIPT

Coating thickness was measured by means of the calotest method. A Hysitron TI 900 Triboindenter device equipped with a Berkovich indenter was employed to measure the hardness and elastic modulus of the coatings. Indentations were performed under applied loads of 5.8 and 10 mN. Poisson ratios of 0.25 and 0.18 were assumed to calculate the elastic modulus of TiN and TiAlN, respectively [17, 18]. Coating adhesion was evaluated by means of scratch tests performed on a CSM Revetest scratch-tester equipped with a Rockwell indenter. The coatings were tested using a progressive load ranging from 1 to 100 N, a loading rate of 99 N/min, a speed of 5 mm/min and a scratch length of 5 mm. Three tests were performed on each coating variant. Critical loads were determined by post-tests optical microscopy. Two stages in the coating damage were considered, the first delamination within the track (Lc1) and massive delamination (Lc2) [19]. The evolution of the friction coefficients during the scratch tests was also evaluated.

Residual stress measurements were also conducted by XRD using the $\sin^2\psi$ method. The optimal diffraction peaks for measurements on the uncoated and coated samples were Fe-α (222), TiN (422) and TiAlN (422), respectively. The 2θ angle ranged from 134° to 140° for Fe-α, from 120° to 132° for TiN and from 122° to 134° for TiAlN. The x-ray elastic constants (XEC's) of the coatings were calculated by utilizing the experimentally determined elastic modules and the assumed Poisson's ratios. Residual stresses in uncoated and coated samples were measured in the perpendicular direction to the grinding scratches.

2.4. Rolling contact fatigue tests

ACCEPTED MANUSCRIPT

RCF tests were performed in a flat washer type testing rig using lubricated pure rolling conditions. Figure 1 provides a schematic view of the testing rig. A 51107 thrust ball bearing was used as a counterpart. This bearing has 21 balls made of SAE 52100 steel with 6 mm in diameter, rolling in a circular track of 44 mm in diameter. The rotational speed of the samples was set at 1650 rpm, establishing a loading frequency of $1x10^6$ cycles/hour. A commercial hydraulic oil with a kinematic viscosity of 100 cSt at 40 °C was used as lubricant. The maximum contact pressure (p_0) was set at 1400 MPa.

Five RCF tests were carried out for each sample set. The samples were loaded until a macroscopic fatigue failure was produced on their surface or until reaching 200 hours of operation without failures. The time to failure of the samples was measured by an hour meter and converted into loading cycles. The rolling track of the samples was examined by SEM and EDS.

RCF results were analyzed using the two-parameter Weibull distribution. Life data were fitted by rank regression [20] and also subjected to a statistical analysis in order to make inferences. For purposes of comparison, the 10 % life (L10) was used. Two-sided 90 % confidence intervals for each sample set were determined by the Weibayes Method [20, 21], assuming the Weibull shape parameter (β) in the Weibayes solution.

3. Results and discussion

3.1. Substrate and coatings characteristics

ACCEPTED MANUSCRIPT

The XRD diffraction patterns of the coated samples, shown in Figure 2, reveal the main diffraction peaks of the coatings together with some substrate peaks, due to the penetration depth of the x-rays is greater than the coating thicknesses. The bilayer Ti/TiN coating has the main diffraction peaks of TiN, Fig.2 (a), having a cubic-NaCl type structure, which grew with a preferred orientation of (111) planes parallel to the samples surface. The patterns of the bilayer TiAl/TiAlN coatings, Fig.2 (b), revealed the main diffraction peaks of TiAlN, also with a cubic-NaCl type structure and with a preferred (111) orientation. In addition, no TiN, AlN or TiAl peaks were recorded for the TiAl/TiAlN coatings. On the other hand, it can be seen that the TiAlN peaks are shifted to higher 2θ angles than TiN peaks. This behaviour is ascribed to the addition of Al into the TiN lattice which causes a decrease in the TiAlN lattice parameter since the atomic size of Al is smaller than Ti [12-14]. The calculated lattice parameters were 4.27 ± 0.01 Å for TiN and 4.20 ± 0.01 Å for TiAlN.

The arithmetic average roughness, surface hardness and surface residual stresses of the uncoated and coated samples are listed in Table 1. Uncoated samples have an average Ra value of 0.17 µm, an average surface hardness of 690 $HK_{0.015}$ (≈ 420 $HBW_{2.5/187.5}$) and compressive surface residual stresses with an average value of 0.26 GPa. According to a previous work [22], ADI residual stresses vary according to the measurement direction, being smaller perpendicular to the grinding marks. The Ra values of the coated samples are close to each other and are higher than the value of uncoated ADI due to the presence of macroparticles (protrusions) in the coatings [23, 24]. The surface hardness of the

ACCEPTED MANUSCRIPT

TiAl/TiAlN coated samples is significantly higher than that of the Ti/TiN coated samples which, in turn, is slightly higher than that of uncoated ADI. The surface residual stresses of the coated samples are also compressive, with average values of 3.65 and 5.20 GPa for the Ti/TiN and TiAl/TiAlN samples, respectively. According to a previous work [22], the residual stresses of the coated samples are independent of the measurement direction indicating a rotationally symmetric stress state. An increase in the stress level by the addition of a third element in a binary coating has been previously reported by other authors [25-28].

The thickness, hardness, elastic modulus and critical loads of the Ti/TiN and TiAl/TiAlN coatings are listed in Table 2. The thickness of the Ti/TiN coatings turned out to be close to 1 µm while that of the TiAl/TiAlN coatings turned out to be higher, with an average value of 1.37 µm. The actual deposition rates turned out to be 0.017 and 0.023 µm/min for Ti/TiN and TiAl/TiAlN coatings, respectively. This difference can be ascribed to the estimation uncertainty, since deposition rate is difficult to control with accuracy in an industrial device. The coating hardness and elastic modulus are higher for TiAl/TIAlN as expected. The values are in agreement with the ranges reported in the literature [12, 18, 29-31]. The higher hardness and stress level of TiAl/TIAlN coatings can be ascribed to the addition of Al into the TiN lattice, which increases the number and/or volume of defects created during film growth, hindering the dislocations movement and inducing strain in the film [26-28, 32]. Regarding the scratch tests results, it can be seen that the average loads at the first delamination within the track (Lc1) are higher for the Ti/TiN coatings while the average loads at massive delamination (Lc2) are quite similar for both coating

ACCEPTED MANUSCRIPT

variants. Figure 3 shows typical tracks resulting from the scratch tests together with the different coating damage stages.

Figure 4 shows the friction coefficient evolution for the coated samples as a function of the scratch length. It can be seen that the behavior of both coating variants is quite similar. Before reaching Lc1 both coatings are undamaged, the friction coefficients are lower than 0.2 and the curves overlap. Between Lc1 and Lc2 both friction coefficients increase markedly and some sharp peaks can be seen in the curves which are related to the fracture and delamination of the coating material [33]. After reaching Lc2 the indenter scratches the substrates, consequently the curves tend to overlap again and the friction coefficients reach values close to 0.6, which correspond to the friction coefficient of the diamond tip against the ADI substrates.

3.2. Rolling contact fatigue behavior

Failures in uncoated ADI samples were characterized by the typical concentrated damage in the form of spalls. Failures in Ti/TiN and TiAl/TiAlN coated samples were also characterized by substrate spalling. Figure 5 shows the failures produced in the coated samples. The rolling direction (RD) is indicated on the micrographs. In Fig. 5b it can be seen some localized delamination around the RCF spall in the TiAl/TiAlN coated sample, however, no massive coating delamination was observed during the RCF tests for both coating variants. Figure 6 exhibits some substrate cracks around the RCF spalls. It can be seen that cracks propagate connecting graphite nodules. Figure 7 shows the Weibull plot

ACCEPTED MANUSCRIPT

of failure probability versus number of loading cycles for the uncoated and coated samples.

The results of the Weibull analysis are summarized in Table 3, reflecting shape parameter (β), characteristic life or scale parameter (η) and coefficient of determination (R^2). It can be seen that the characteristic life of the uncoated and coated samples can be ranked as follows: ADI-Ti/TiN > ADI-TiAl/TiAlN > ADI. This behavior would indicate, in principle, that the application of both coating variants improves the RCF resistance of ADI.

Table 4 compares the Weibull and Weibayes estimates of L10 for the uncoated and coated samples as a validity check of the Weibayes solution. Two-sided 90 % confidence intervals, determined by the Weibayes Method, are also reported. It can be seen that both solutions provide similar values of L10 for each sample set confirming the validity of the Weibayes solution. In addition, the L10 estimates of the uncoated and coated samples confirm the tendency observed for the η values. However, the estimated confidence intervals indicate that there are no significant differences between the RCF resistance of the uncoated and TiAl/TiAlN coated samples while the RCF resistance of the Ti/TiN coated samples is noticeably higher. This behavior can be ascribed to the fact that a coating with small mismatch of properties with respect to the substrate provides a better distribution of contact stresses than a coating with higher values of those properties [33-35]. Therefore, a deformation of the coating without cracking and/or delamination and a reduction of the contact stresses within the substrate, with the consequent increase of the RCF life, are likely to occur.

ACCEPTED MANUSCRIPT

4. Conclusions

Ti/TiN and TiAl/TiAlN bilayer coatings were applied onto ADI samples by CAD using an industrial device. TiN and TiAlN coatings grew with a cubic-NaCl type structure and a preferred orientation of (111) planes parallel to the samples surface. The arithmetic average roughness, the critical loads at massive delamination and the evolution of the friction coefficients are quite similar for both coating variants. The surface residual stresses are compressive. The surface hardness and residual stresses are higher for the TiAl/TIAlN coated samples. The coating hardness and elastic modulus are also higher for TiAl/TIAlN while the critical loads at the first delamination within the track are higher for Ti/TiN.

Regarding RCF, failures in Ti/TiN and TiAl/TiAlN coated samples were characterized by substrate spalling. No massive coating delamination was observed during the tests. The η and L10 estimates of the uncoated and coated samples can be ranked as follows: ADI-Ti/TiN > ADI-TiAl/TiAlN > ADI. The estimated confidence intervals indicate that the deposition of Ti/TiN improves noticeably the RCF resistance of ADI while the deposition of TiAl/TiAlN does not produce significant changes. The higher RCF resistance of the Ti/TiN coated samples can be ascribed to the smaller mismatch of properties between substrate and coating as compared to TiAl/TiAlN, owing to the fact that a relatively softer and more compliant coating provides, on the one hand, a better distribution of contact stresses during RCF cycles and, on the other, a higher capacity to withstand deformations without cracking and/or delamination.

ACCEPTED MANUSCRIPT

Acknowledgments

The financial support granted by the CONICET (Grant No. PIP 11220120100468CO), the ANPCYT (Grant No. PICT 2013-2630) and the National University of Mar del Plata (Grant No. 15/G394) is gratefully acknowledged.

References

[1] D.A. Colombo, M.D. Echeverría, S. Laino, R.C. Dommarco, J.M. Massone, Rolling contact fatigue resistance of PVD CrN and TiN coated austempered ductile iron, Wear 308 (2013) 35-45.

[2] D.A. Colombo, M.D. Echeverría, R.C. Dommarco, J.M. Massone, Influence of TiN coating thickness on the rolling contact fatigue resistance of austempered ductile iron, Wear 350–351 (2016) 82-88.

[3] D.A. Colombo, J.M. Massone, M.D. Echeverría, A.B. Márquez, Rolling contact fatigue behavior of Ti/TiN coated ADI by cathodic arc deposition, Ceram. Int. 43 (2017) 4263-4271.

[4] V. Chawla, R. Jayaganthan, R. Chandra, A study of structural and mechanical properties of sputter deposited nanocomposite Ti–Si–N thin films, Surf. Coat. Technol. 204 (2010) 1582-1589.

ACCEPTED MANUSCRIPT

[5] A. Hoerling, J. Sjölén, H. Willmann, T. Larsson, M. Odén, L. Hultman, Thermal stability, microstructure and mechanical properties of Ti1−xZrxN thin films, Thin Solid Films 516 (2008) 6421-6431.

[6] A. Hörling, L. Hultman, M. Odén, J. Sjölén, L. Karlsson, Mechanical properties and machining performance of Ti1−xAlxN-coated cutting tools, Surf. Coat. Technol. 191 (2005) 384-392.

[7] D.E. Wolfe, B.M. Gabriel, M.W. Reedy, Nanolayer (Ti,Cr)N coatings for hard particle erosion resistance, Surf. Coat. Technol. 205 (2011) 4569-4576.

[8] Y.C. Chim, X.Z. Ding, X.T. Zeng, S. Zhang, Oxidation resistance of TiN, CrN, TiAlN and CrAlN coatings deposited by lateral rotating cathode arc, Thin Solid Films 517 (2009) 4845-4849.

[9] J. Deng, F. Wu, Y. Lian, Y. Xing, S. Li, Erosion wear of CrN, TiN, CrAlN, and TiAlN PVD nitride coatings, International Journal of Refractory Metals and Hard Materials 35 (2012) 10-16.

[10] S.-Y. Yoon, K.O. Lee, S.S. Kang, K.H. Kim, Comparison for mechanical properties between TiN and TiAlN coating layers by AIP technique, J. Mater. Process. Technol. 130–131 (2002) 260-265.

[11] L. Chen, J. Paulitsch, Y. Du, P.H. Mayrhofer, Thermal stability and oxidation resistance of Ti–Al–N coatings, Surf. Coat. Technol. 206 (2012) 2954-2960.

[12] S. PalDey, S.C. Deevi, Single layer and multilayer wear resistant coatings of (Ti,Al)N: a review, Mater. Sci. Eng., A 342 (2003) 58-79.

ACCEPTED MANUSCRIPT

[13] A. Kimura, M. Kawate, H. Hasegawa, T. Suzuki, Anisotropic lattice expansion and shrinkage of hexagonal TiAlN and CrAlN films, Surf. Coat. Technol. 169–170 (2003) 367-370.

[14] M. Zhou, Y. Makino, M. Nose, K. Nogi, Phase transition and properties of Ti–Al–N thin films prepared by r.f.-plasma assisted magnetron sputtering, Thin Solid Films 339 (1999) 203-208.

[15] D.A. Colombo, M.D. Echeverría, O.J. Moncada, J.M. Massone, Characterisation of PVD–TiN coated austempered ductile iron: effects of nodule count and austempering temperature, ISIJ Int. 51 (2011) 448-455.

[16] D.A. Colombo, M.D. Echeverría, O.J. Moncada, J.M. Massone, PVD TiN and CrN coated austempered ductile iron: analysis of processing parameters influence on coating characteristics and substrate microstructure, ISIJ Int. 52 (2012) 121-126.

[17] H. Ljungcrantz, M. Oden, L. Hultman, J.E. Greene, J.E. Sundgren, Nanoindentation studies of single-crystal (001)-, (011)-, and (111)-oriented TiN layers on MgO, J. Appl. Phys. 80 (1996) 6725-6733.

[18] E. Vogli, W. Tillmann, U. Selvadurai-Lassl, G. Fischer, J. Herper, Influence of Ti/TiAlN-multilayer designs on their residual stresses and mechanical properties, Appl. Surf. Sci. 257 (2011) 8550-8557.

[19] Y.X. Ou, J. Lin, S. Tong, W.D. Sproul, M.K. Lei, Structure, adhesion and corrosion behavior of CrN/TiN superlattice coatings deposited by the combined deep oscillation magnetron sputtering and pulsed dc magnetron sputtering, Surf. Coat. Technol. 293 (2016) 21-27.

ACCEPTED MANUSCRIPT

[20] R.B. Abernethy, The New Weibull Handbook, 4th Edition ed., R.B. Abernethy, Florida, USA, 2000.

[21] J.I. McCool, Using the Weibull Distribution: Reliability, Modeling and Inference, Wiley, New Yersey, USA, 2012.

[22] D.A. Colombo, M.D. Echeverría, O.J. Moncada, J.M. Massone, Residual stress analysis in PVD coated austempered ductile iron, ISIJ Int. 53 (2013) 520-526.

[23] J.-W. Lee, J.-G. Duh, J.-H. Wang, Mechanical property evaluation of cathodic arc plasma-deposited CrN thin films on Fe-Mn-Al-C alloys, Surf. Coat. Technol. 168 (2003) 223-230.

[24] M.-H. Shiao, F.-S. Shieu, A formation mechanism for the macroparticles in arc ion-plated TiN films, Thin Solid Films 386 (2001) 27-31.

[25] L. Karlsson, A. Hörling, M.P. Johansson, L. Hultman, G. Ramanath, The influence of thermal annealing on residual stresses and mechanical properties of arc-evaporated TiCxN1−x (x=0, 0.15 and 0.45) thin films, Acta Mater. 50 (2002) 5103-5114.

[26] L. Karlsson, L. Hultman, M.P. Johansson, J.E. Sundgren, H. Ljungcrantz, Growth, microstructure, and mechanical properties of arc evaporated TiCxN1−x (0≤x≤1) films, Surf. Coat. Technol. 126 (2000) 1-14.

[27] L. Karlsson, L. Hultman, J.E. Sundgren, Influence of residual stresses on the mechanical properties of TiCxN1–x (x=0, 0.15, 0.45) thin films deposited by arc evaporation, Thin Solid Films 371 (2000) 167-177.

ACCEPTED MANUSCRIPT

[28] A.E. Reiter, V.H. Derflinger, B. Hanselmann, T. Bachmann, B. Sartory, Investigation of the properties of Al1−xCrxN coatings prepared by cathodic arc evaporation, Surf. Coat. Technol. 200 (2005) 2114-2122.

[29] L. Chen, Y. Yang, M.J. Wu, Y.X. Xu, Y. Du, S. Kolozsvári, Correlation between arc evaporation of Ti–Al–N coatings and corresponding Ti0.50Al0.50 target types, Surf. Coat. Technol. 275 (2015) 309-315.

[30] F. Cai, S. Zhang, J. Li, Z. Chen, M. Li, L. Wang, Effect of nitrogen partial pressure on Al–Ti–N films deposited by arc ion plating, Appl. Surf. Sci. 258 (2011) 1819-1825.

[31] F. Cai, M. Chen, M. Li, S. Zhang, Influence of negative bias voltage on microstructure and property of Al-Ti-N films deposited by multi-arc ion plating, Ceram. Int. 43 (2017) 3774-3783.

[32] H. Makoto, U. Yasuhiro, S. Tsuneo, J. Weihua, G. Constantin, Y. Kiyoshi, Characteristics of (Cr 1- x , Al x)N Films Prepared by Pulsed Laser Deposition, Japanese Journal of Applied Physics 40 (2001) 1056.

[33] X. Huang, I. Etsion, T. Shao, Effects of elastic modulus mismatch between coating and substrate on the friction and wear properties of TiN and TiAlN coating systems, Wear 338-339 (2015) 54-61.

[34] L. Qin, C. Li, S. Chen, C. Liu, B. Tang, Improving load-bearing property of hard thin film on soft substrate by elastic modulus distribution design, Mater. Lett. 110 (2013) 215-217.

[35] C.T. Wang, T.J. Hakala, A. Laukkanen, H. Ronkainen, K. Holmberg, N. Gao, R.J.K. Wood, T.G. Langdon, An investigation into the effect of substrate on the load-bearing capacity of thin hard coatings, J. Mater. Sci. 51 (2016) 4390-4398.

ACCEPTED MANUSCRIPT

Table captions

Table 1. Properties of the uncoated and coated samples

Table 2. Properties of the Ti/TiN and TiAl/TiAlN coatings

Table 3. Estimates of the Weibull parameters for the uncoated and coated samples

Table 4. Weibull and Weibayes estimates of L10 for the uncoated and coated samples and 90 % confidence intervals

Figure Captions

Figure 1. Schematic view of the flat washer RCF testing rig

Figure 2. XRD patterns of the coated samples: (a) ADI-Ti/TiN, (b) ADI-TiAl/TiAlN

Figure 3. Representative images of the scratch tests tracks: (a) ADI-Ti/TiN, (b) ADI-TiAl/TiAlN

Figure 4. Friction coefficient evolution for the different coating variants analyzed

Figure 5. RCF failures in coated samples: (a) ADI-Ti/TiN, (b) ADI-TiAl/TiAlN

Figure 6. Substrate cracks around the RCF spalls

Figure 7. Weibull plot for the uncoated and coated samples

ACCEPTED MANUSCRIPT

ACCEPTED MANUSCRIPT

Table 1

Sample	Arithmetic average roughness, Ra (μm)	Surface hardness ($HK_{0.015}$)	Surface residual stresses (GPa)
ADI	0.17 ± 0.02	690 ± 67	-0.26 ± 0.05
ADI-Ti/TiN	0.28 ± 0.02	838 ± 73	-3.65 ± 0.38
ADI-TiAl/TiAlN	0.27 ± 0.02	1910 ± 97	-5.20 ± 0.67

ACCEPTED MANUSCRIPT

ACCEPTED MANUSCRIPT

Table 2

Sample	Coating Thickness (μm)	Hardness (GPa)	Elastic modulus (GPa)	Critical loads (N)	
				Lc1	Lc2
ADI-Ti/TiN	0.99 ± 0.07	25.5 ± 4.2	278 ± 25	28.8 ± 1.1	52.7 ± 6.6
ADI-TiAl/TiAlN	1.37 ± 0.02	37.4 ± 6.8	401 ± 52	23.2 ± 1.7	44.8 ± 5.0

ACCEPTED MANUSCRIPT

ACCEPTED MANUSCRIPT

Table 3

Sample	β	η (cycles x10^6)	R^2
ADI	4.54	84.89	0.902
ADI-Ti/TiN	4.61	150.2	0.911
ADI-TiAl/TiAlN	5.39	97.54	0.962

ACCEPTED MANUSCRIPT

ACCEPTED MANUSCRIPT

Table 4

Sample	Weibull Estimate (cycles x10^6)	Weibayes Estimate (cycles x10^6)	Weibayes confidence interval (cycles x10^6)
ADI	51.71	50.03	43.79 – 61.42
ADI-Ti/TiN	92.16	91.01	79.82 – 111.4
ADI-TiAl/TiAlN	64.25	62.83	56.17 – 74.69

ACCEPTED MANUSCRIPT

ACCEPTED MANUSCRIPT

Highlights

- Hardness, elastic modulus and residual stresses are higher for TiAl/TIAlN films
- Critical loads and friction coefficients are quite similar for both coating variants
- Wear was assessed by means of rolling contact fatigue (RCF) tests
- RCF failures in coated samples were characterized exclusively by substrate spalling
- RCF resistance can be ranked as follows: ADI-Ti/TiN > ADI-TiAl/TiAlN ≈ ADI

ACCEPTED MANUSCRIPT

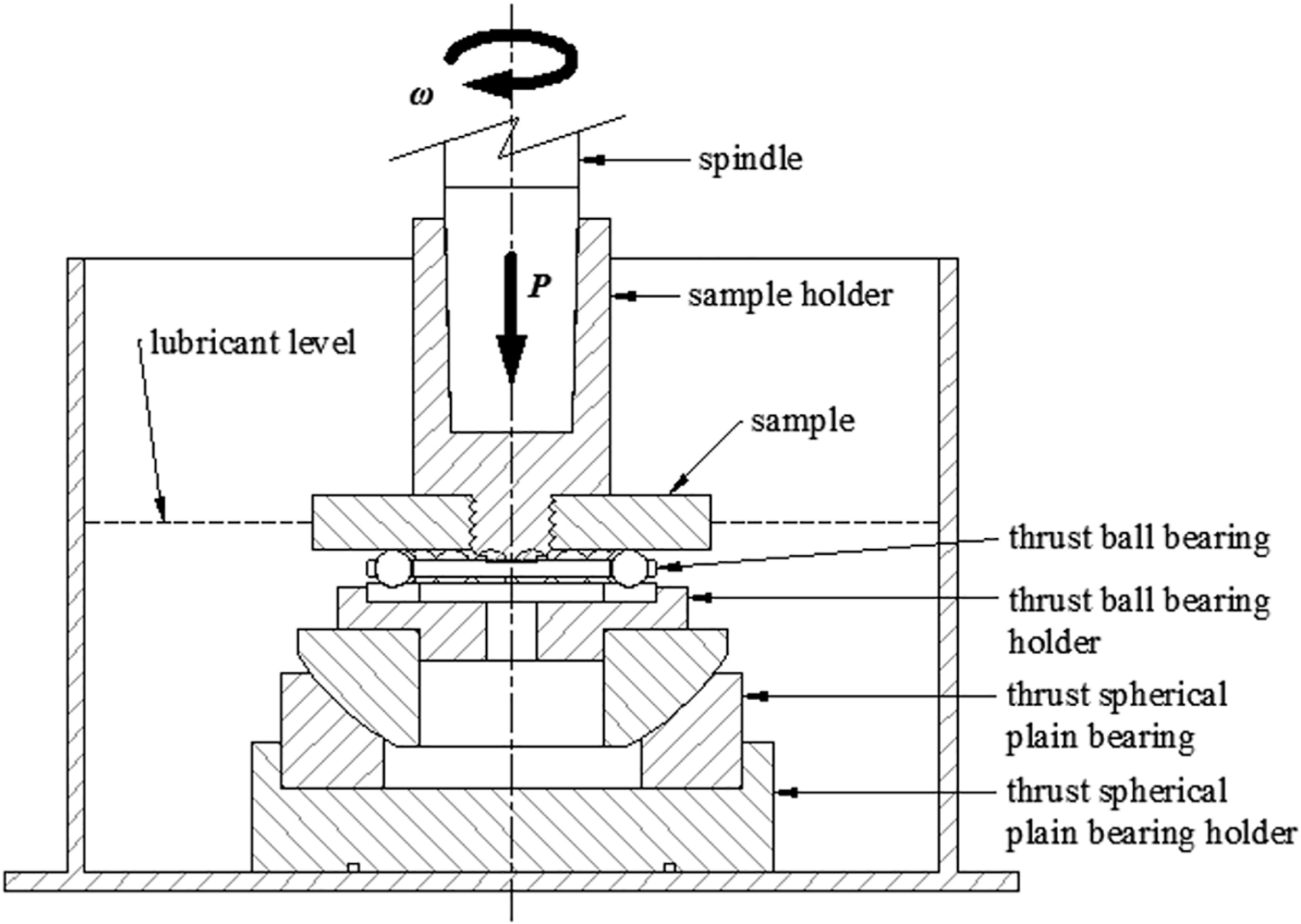
ω
spindle
P
sample holder
lubricant level
sample
thrust ball bearing
thrust ball bearing holder
thrust spherical plain bearing
thrust spherical plain bearing holder

Figure 1

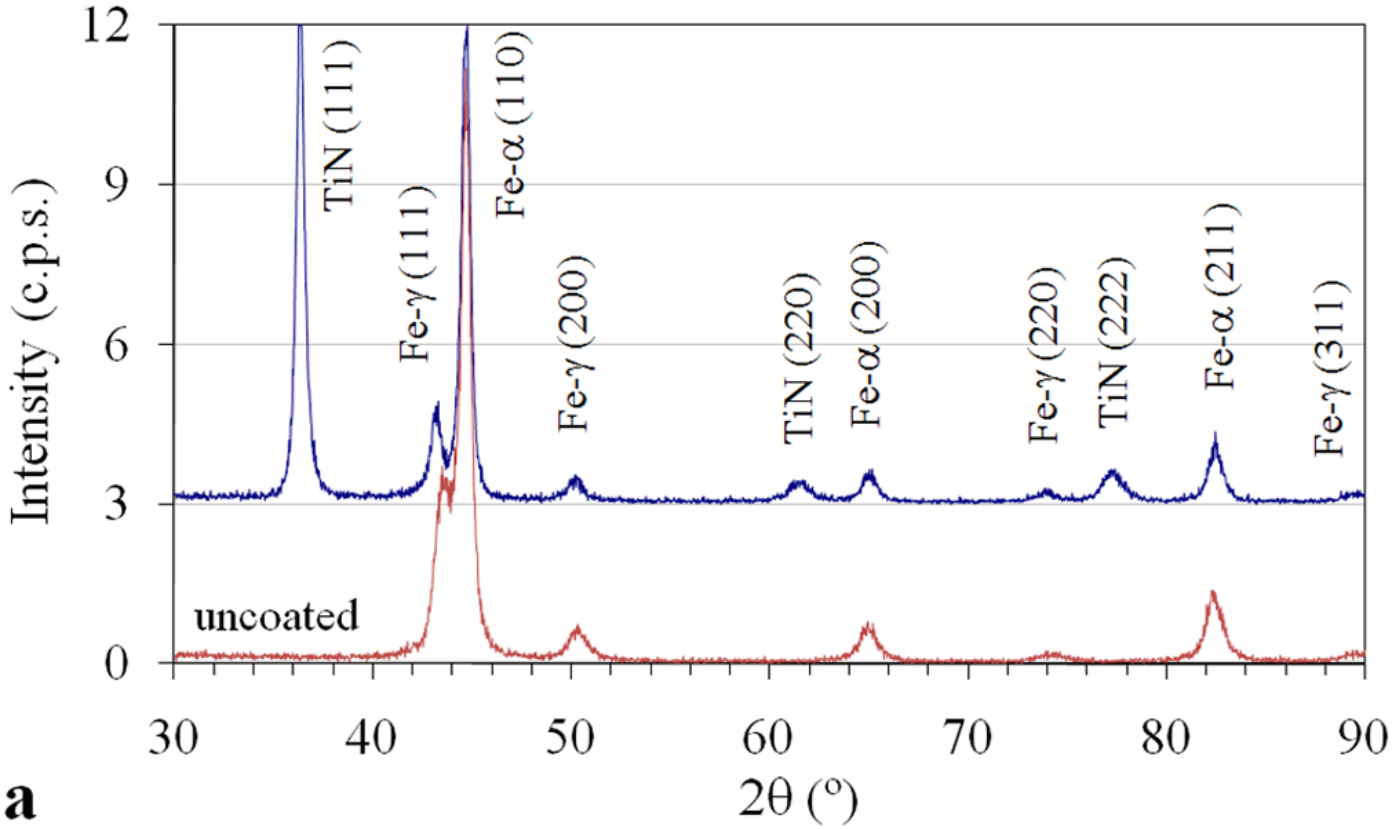
Intensity (c.p.s.)
12
9
6
3
0
TiN (111)
Fe-γ (111)
Fe-α (110)
Fe-γ (200)
TiN (220)
Fe-α (200)
Fe-γ (220)
TiN (222)
Fe-α (211)
Fe-γ (311)
uncoated
30
40
50
60
70
80
90
2θ (°)
a

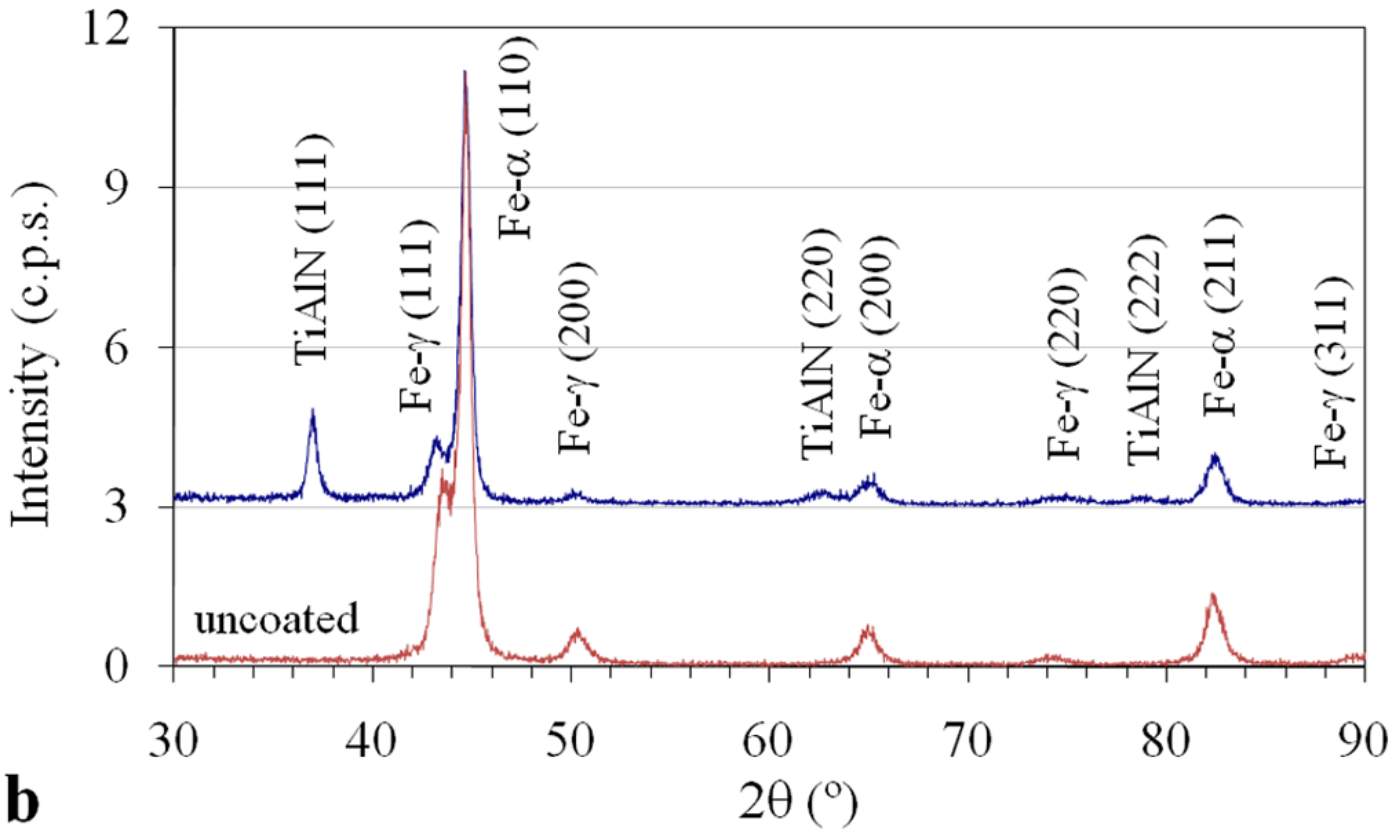
Intensity (c.p.s.)
12
9
6
3
0
TiAlN (111)
Fe-γ (111)
Fe-α (110)
Fe-γ (200)
TiAlN (220)
Fe-α (200)
Fe-γ (220)
TiAlN (222)
Fe-α (211)
Fe-γ (311)
uncoated
30
40
50
60
70
80
90
2θ (°)
b

Figure 2

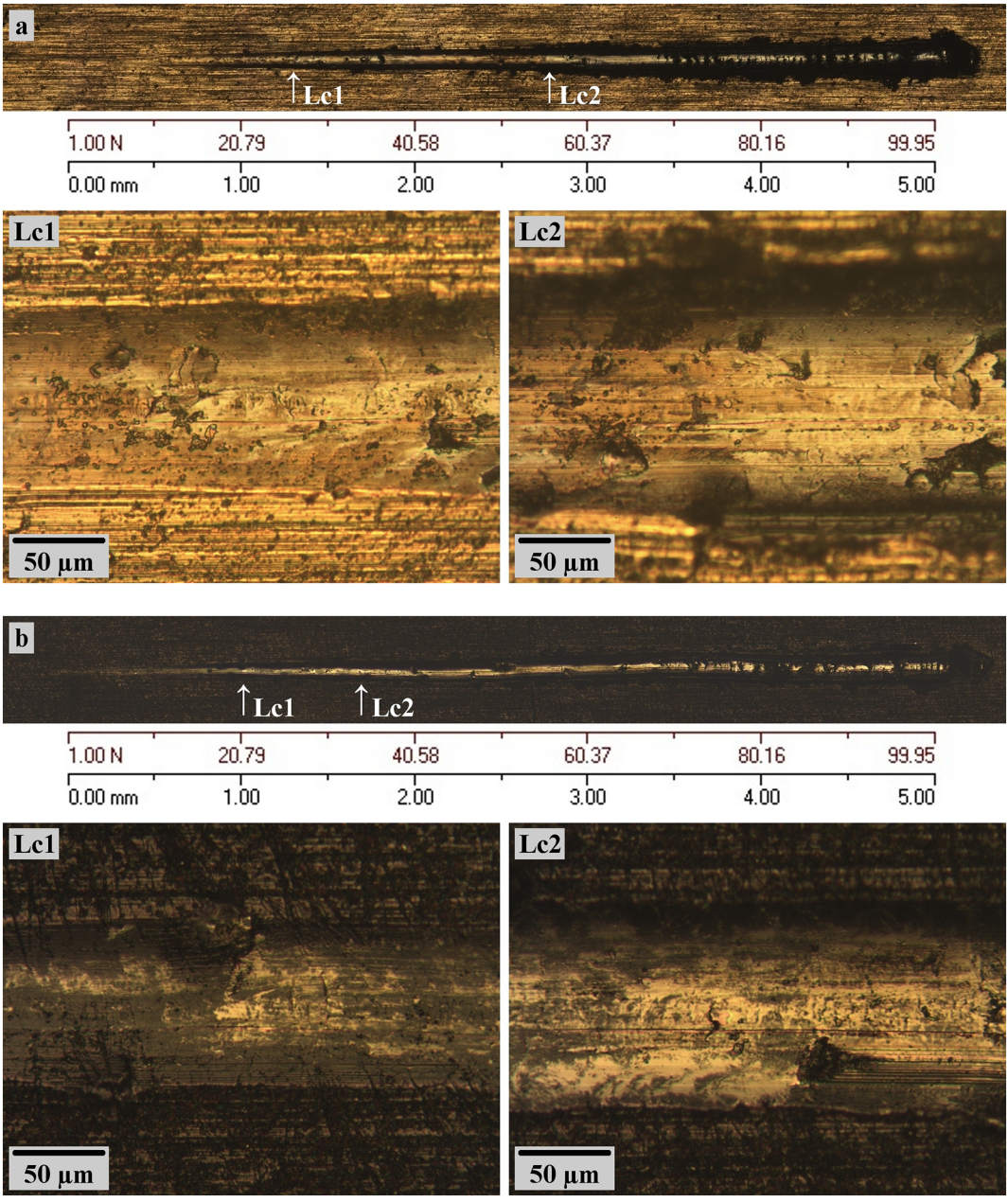
a
Lc1
Lc2
1.00 N
20.79
40.58
60.37
80.16
99.95
0.00 mm
1.00
2.00
3.00
4.00
5.00
Lc1
50 µm
Lc2
50 µm
b
Lc1
Lc2
1.00 N
20.79
40.58
60.37
80.16
99.95
0.00 mm
1.00
2.00
3.00
4.00
5.00
Lc1
50 µm
Lc2
50 µm

Figure 3

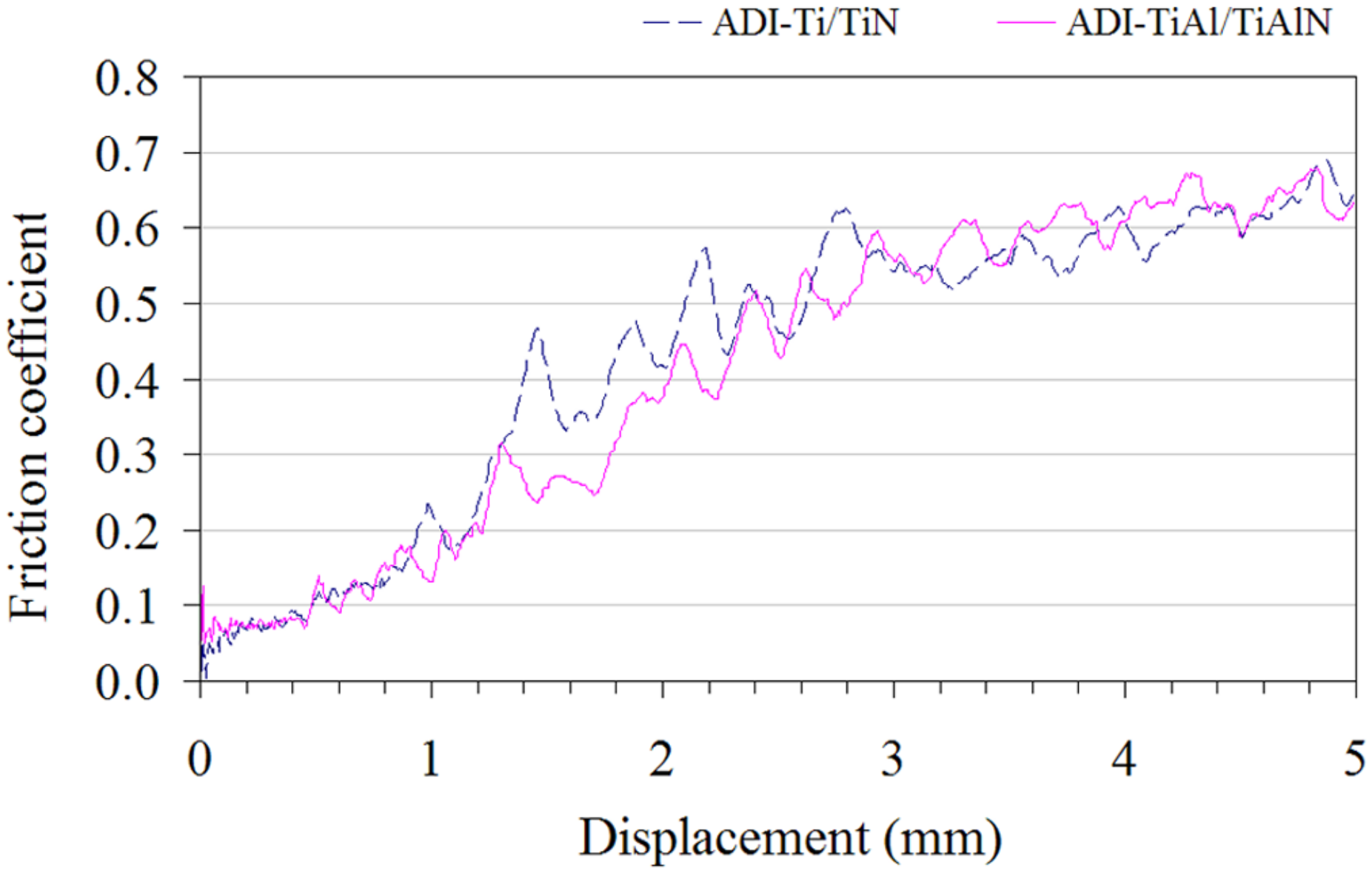
ADI-Ti/TiN
ADI-TiAl/TiAlN
Friction coefficient
0.0
0.1
0.2
0.3
0.4
0.5
0.6
0.7
0.8
0
1
2
3
4
5
Displacement (mm)

Figure 4

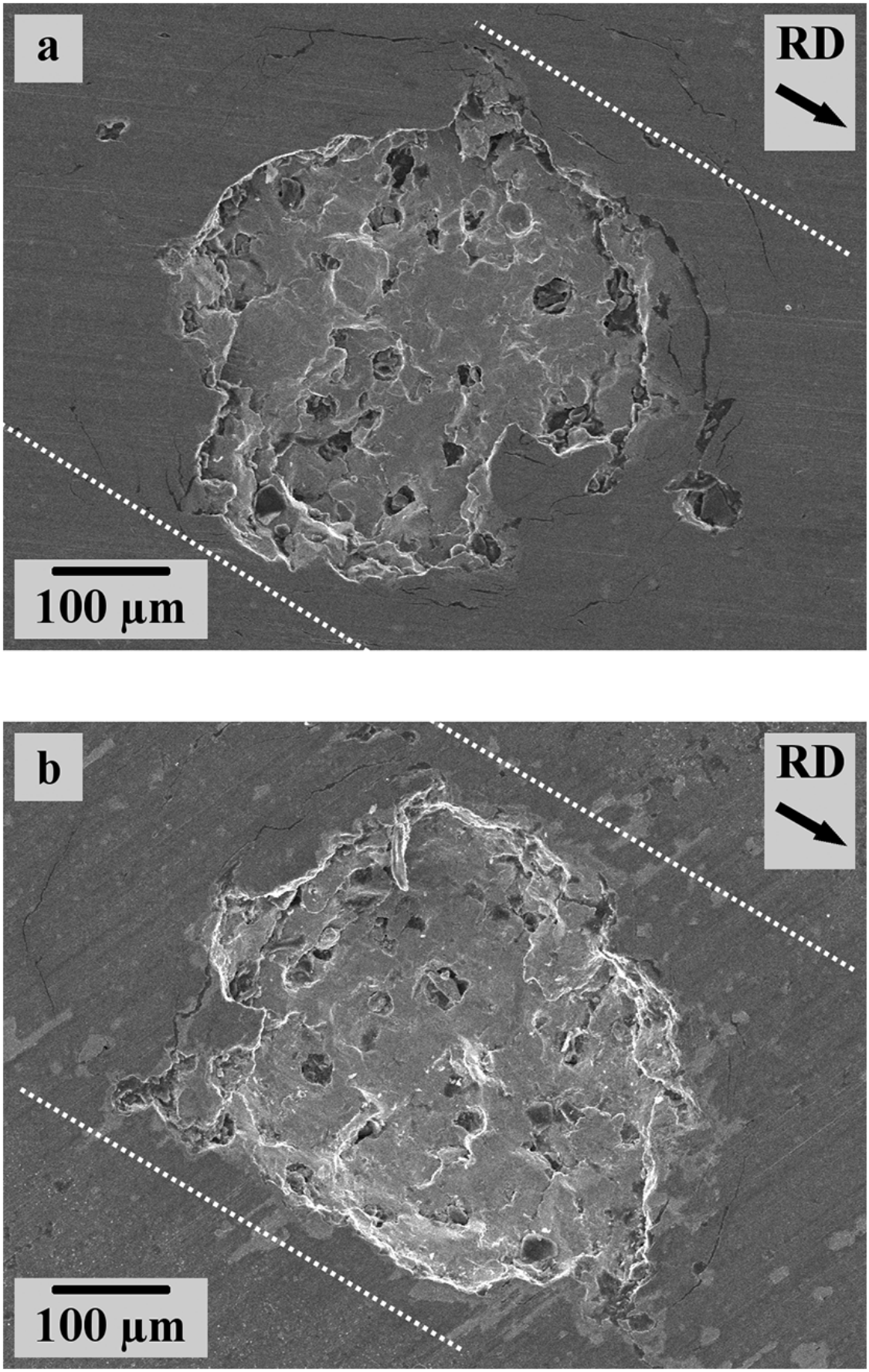

Figure 5

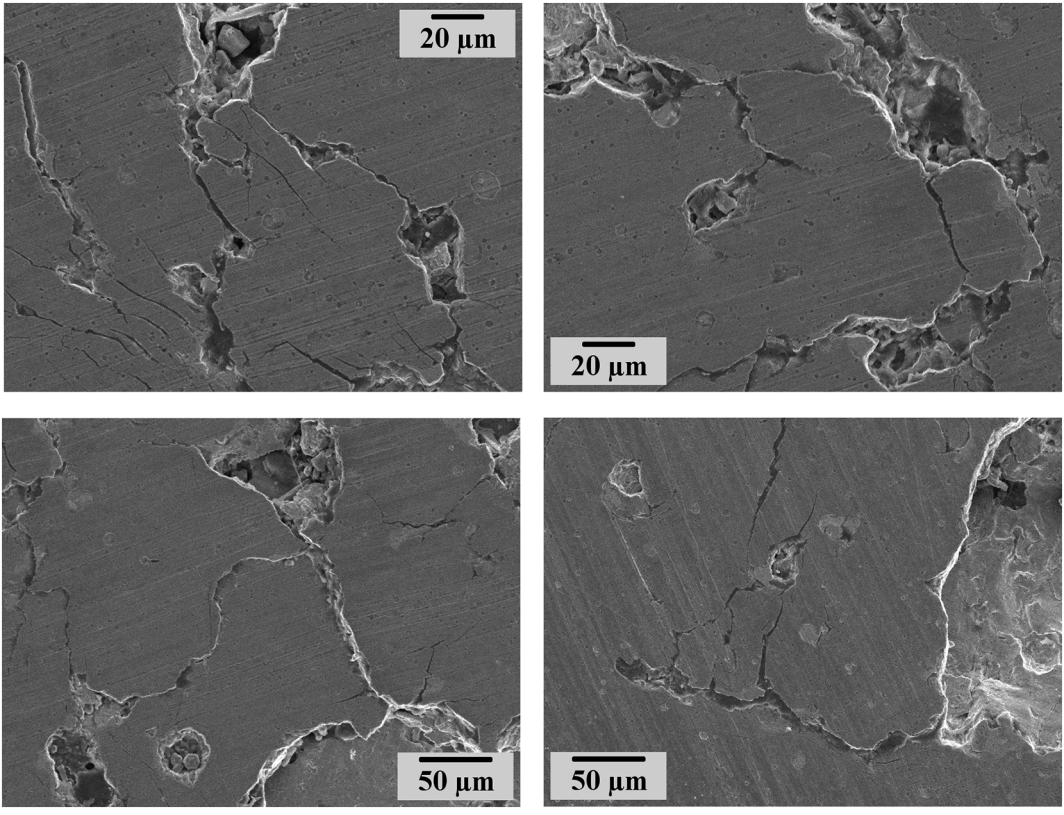

Figure 6

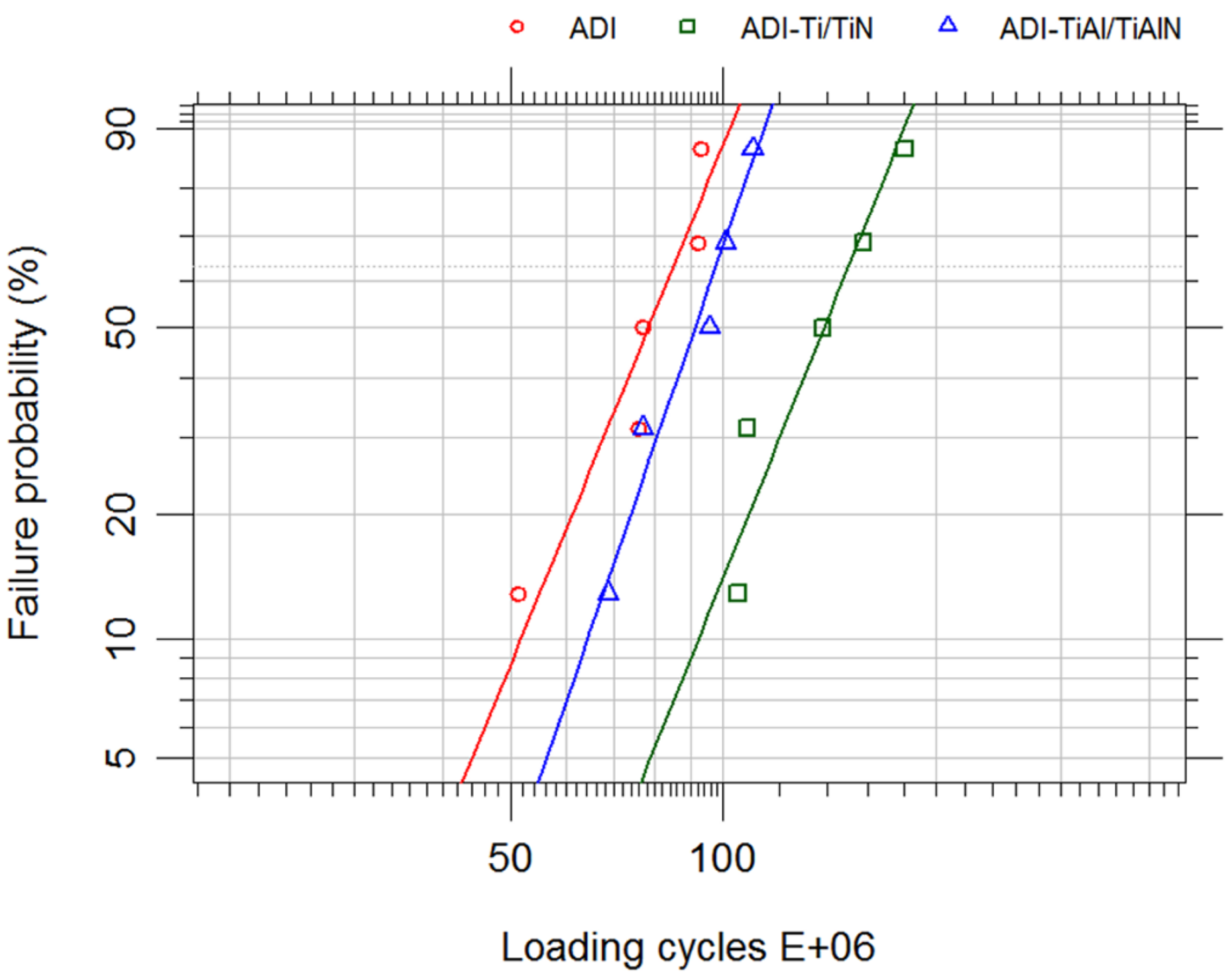
ADI
ADI-Ti/TiN
ADI-TiAl/TiAlN
Failure probability (%)
90
50
20
10
5
50
100
Loading cycles E+06

Figure 7